

## Optical properties and possible sources of brown carbon in PM<sub>2.5</sub> over Xi'an, China



Zhenxing Shen<sup>a, b, \*</sup>, Qian Zhang<sup>a</sup>, Junji Cao<sup>b</sup>, Leiming Zhang<sup>c</sup>, Yali Lei<sup>a</sup>, Yu Huang<sup>b</sup>, R.-J. Huang<sup>b</sup>, Jinjin Gao<sup>a</sup>, Zhuzi Zhao<sup>b</sup>, Chongshu Zhu<sup>b</sup>, Xiuli Yin<sup>d</sup>, Chunli Zheng<sup>a</sup>, Hongmei Xu<sup>a</sup>, Suixin Liu<sup>a</sup>

<sup>a</sup> Department of Environmental Science and Engineering, Xi'an Jiaotong University, Xi'an, 710049, China

<sup>b</sup> Key Lab of Aerosol Chemistry & Physics, Institute of Earth Environment, Chinese Academy of Sciences, Xi'an, 710049, China

<sup>c</sup> Air Quality Research Division, Science and Technology Branch, Environment and Climate Change Canada, Toronto, Canada

<sup>d</sup> Guangzhou Institute of Energy Conversion, Chinese Academy of Sciences, 510640, China

### HIGHLIGHTS

- Light absorption of brown carbon (BrC) in PM<sub>2.5</sub> was investigated.
- Biomass burning is an important source for winter BrC.
- Secondary BrC was mainly fresh SOC in winter and aged one in summer.

### ARTICLE INFO

#### Article history:

Received 22 September 2016

Received in revised form

7 November 2016

Accepted 9 November 2016

Available online 11 November 2016

#### Keywords:

Brown carbon

Absorption coefficient

Mass absorption coefficient

Secondary organic carbon

### ABSTRACT

To quantify optical and chemical properties of PM<sub>2.5</sub> brown carbon (BrC) in Xi'an, 58 high-volume ambient PM<sub>2.5</sub> samples were collected during 2 November 2009 to 13 October 2010. Mass concentrations of chemical components were determined, including water-soluble ions, water-soluble organic carbon, levoglucosan, organic carbon (OC), and element carbon (EC). BrC, as an unidentified and wavelength-dependent organic compound, was also measured from water-soluble carbon (WSOC) at 340 nm using UV–vis spectrometer. The wavelength-dependent absorption coefficient ( $b_{\text{abs}}$ ) and mass absorption coefficient (MAC) were much abundant at 340 nm, and the high Absorption Ångström coefficient (AAC) values were observed around 5.4, corresponding to the existence of BrC in ambient PM<sub>2.5</sub>, especially in winter. Good correlations ( $R > 0.60$ ) between  $b_{\text{abs}}$  and biomass burning markers, such as levoglucosan and  $\text{K}^+$ , in winter indicated significant amounts of primary BrC from biomass burning emissions. Secondary organic carbon BrC (SOC–BrC) was more abundant in winter than in summer. SOC–BrC in winter was mainly fresh SOC formed from aqueous phase reactions while in summer, aged SOC from photo-chemical formation. Source profiles of BrC optical parameters were detected, which verified sources of BrC from biomass burning and coal burning emissions in areas surrounding Xi'an. The rapidly decreasing  $b_{\text{abs-340nm}}$  values from biomass burning smoldering to straw pellet burning suggested that burning straw pellet instead of burning straw directly is an effective measure for reducing BrC emissions.

© 2016 Elsevier Ltd. All rights reserved.

### 1. Introduction

Light-absorbing carbonaceous aerosols have significant climatic impacts due to their direct and semi-direct aerosol forcing. Black

carbon (BC) is the best-known light-absorbing carbonaceous aerosol at the visible wavelengths (400–700 nm) in the atmosphere, contributing ~71% of total solar energy absorption (Feng et al., 2013). However, there is a growing body of evidence showing that some organic aerosols, which are referred to as “brown carbon (BrC)”, have strong absorption abilities at near-ultraviolet and blue wavelengths and also affect radiative balance (Andreae and Gelencser, 2006; Kirchstetter et al., 2004; Chen and

\* Corresponding author.

E-mail address: [zxshen@mail.xjtu.edu.cn](mailto:zxshen@mail.xjtu.edu.cn) (Z. Shen).

Bond, 2010; Lack et al., 2012). Kirchstetter and Thatcher (2012) showed that wood smoke BrC accounted for 49% of light absorption at wavelengths below 400 nm, illustrating that BrC is only secondary to BC in light absorption and affects tropospheric photochemistry significantly. Unlike wavelength-independent absorption of BC, the light absorption of BrC relates to wavelength closely. Thus, the value of the Absorption Ångström coefficient (AAC), which is referred to as a power exponent of wavelength, is nearly constant (~1) for BC, but ranges from 2 to 7 for BrC (Moosmuller et al., 2011; Srinivas and Sarin, 2014; Hoffer et al., 2006; Chen and Bond, 2010; Bones et al., 2010; Hecobian et al., 2010).

Quantifying the optical properties of BrC often relies on highly sensitive spectrophotometric measurements in liquid samples or from filter extracts in order to avoid interference by insoluble strong absorption materials (such as BC). A strong correlation between BrC and water-soluble organic carbon (WSOC) has been observed in various studies (Hecobian et al., 2010; Kieber et al., 2006; Lukács et al., 2007; Zhang et al., 2011; Srinivas and Sarin, 2014). For example, Hecobian et al. (2010) measured water-soluble organic aerosols and light-absorption characteristics of aqueous extracts over the Southeastern US and identified abundant BrC in WSOC. About 73% of BrC was extracted using water and the light absorption of water soluble BrC is approximately 2 times lower than the actual ambient BrC in previous studies (Liu et al., 2013; Chen and Bond, 2010). BrC was ubiquitous in atmosphere, including primary and secondary BrC, with the former mainly emitted from anthropogenic sources such as smoldering wood and biofuels burning, and the latter produced from photo-oxidation of biomass burning emissions (Chakrabarty et al., 2010; Hoffer et al., 2006; Kirchstetter and Thatcher, 2012; Lack et al., 2012; Lukács et al., 2007; Saleh et al., 2013; Kieber et al., 2006). In addition, Yang et al. (2009) and Bond (2001) measured relatively abundant primary BrC from inefficient burning of coal or other fossil materials (such as residential cooking and heating).

Xi'an, the capital of Shaanxi Province, is the largest city in northwestern China. High loadings of airborne pollutants have been observed in the city, and coal combustion and biomass burning played important roles in winter haze days in this region (Cao et al., 2005, 2007; 2009; Shen et al., 2009). Biomass burning in this area is normally referred to the traditional way of maize straw burning in "Heated Kang" in winter for rural-area residential heating. Maize straw smoldering in "Heated Kang" is a big problem to rural and urban air pollution (Shen et al., 2009; Sun et al., 2017; Zhu et al., 2016). The primary objective of the present study is to reveal the optical characteristics of water-soluble BrC in PM<sub>2.5</sub> samples in Xi'an, and establish the relationship between BrC and other chemical components. Emission source samples (e.g. coal burning, biomass burning, and straw pellet burning) were also collected for identifying specific BrC sources.

## 2. Materials and methods

### 2.1. Site description and data sampling

The sampling site (Fig. 1) is located in the southeastern area of downtown Xi'an, where experiences heavy air pollution produced by surrounding residential areas, school campus and major traffic roads. Ambient PM<sub>2.5</sub> aerosol samples were collected on pre-combustion quartz filters using a high-volume (~1.13 m<sup>3</sup> min<sup>-1</sup>) air sampler (HVS-PM<sub>2.5</sub>, Thermo-Anderson Inc.) at the rooftop of a 15 m high building. A total of 58 daily (24-h starting at 9:30 a.m.) samples was collected from 2 November 2010 to 13 October 2011. Besides, typical combustion sources samples were also collected on

the 47 mm quartz filters by low-volume sampler (Mini-vol) operating at a flow rate of 5 L min<sup>-1</sup> based on the custom-made dilution system with an adjustable dilution rate of 5- to 80-fold. The calibration of each low- and high-volume sampler was conducted using its corresponding calibration orifice (National Institute Standards and Technology (NIST) Traceable Calibration Certificate). Detailed descriptions of dilution system were presented in Tian et al. (2015). The source samples conducted here include (1) maize straw burning in "Heated Kang", (2) coal burning, and (3) straw pellet combustion (compressed cornstalk in cubic block shape for effective burning, referred to as completely biomass burning). To limit the potential evaporation loss of volatile inorganic or organic compounds from the high volume filters, all the filters were previously baked for 3 h at 800 °C in a furnace to remove residue carbon compounds and stored in sealed plastic bags until further use. After sampling, the filters were stored in a freezer at -4 °C to prevent the evaporation of volatile compounds until further analysis. For quality assurance and quality control of the sample collection and analysis, blank filters were also collected for field and laboratory analysis. All the reported PM mass, inorganic and organic compounds have been corrected using field blanks. The same methods were presented in Shen et al. (2009) and Zhang et al. (2015).

### 2.2. PM chemical analysis

Each of the collected ambient filters was punched into circle filter (diameter = 47 mm) for PM chemical composition analysis. Three quarters of each circle filter were dissolved into distilled-deionized water (10, 2.0, and 15 mL) with a resistivity of 18.3 MΩ for separate analysis of water-soluble ions, levoglucosan, and WSOC. Each solvent was sonicated for 1 h and shaken by mechanical shaker for 1 h, and kept at room temperature for 20 h allowing the solution reaching equilibrium. All the extracts were filtered 1–3 times with a 0.45 mm pore size microporous membrane, and then stored at 4 °C in a clean tube until sample analysis. The concentrations of extracts (such as Na<sup>+</sup>, NH<sub>4</sub><sup>+</sup>, K<sup>+</sup>, Mg<sup>2+</sup>, Ca<sup>2+</sup>, F<sup>-</sup>, Cl<sup>-</sup>, NO<sub>3</sub><sup>-</sup>, and SO<sub>4</sub><sup>2-</sup>) were analyzed using an ion chromatography (IC, Dionex 500, Dionex Corp, Sunnyvale, California, United States). Different concentrations of carbohydrate standards were made from stock solutions of solid dissolved in distilled-deionized water and measured three times during the study to calibrate the IC instruments. The method was validated at detection limits of concentration of ≤0.05 mg L<sup>-1</sup> for each measured water-soluble ion. One in each group of ten samples was selected for repeating analysis for quality control purpose and the relative standard deviation (SD) of each ion was less than 5% for the reproducibility test. Detailed description of ions analysis can be found in Shen et al. (2007, 2008).

Levoglucosan concentration was measured by the method of improved high-performance anion-exchange chromatography (HPAEC) with pulsed amperometric detection (PAD). The HPAEC-PAD system was composed of a Dionex ICS-3000 series ion chromatograph (Dionex Corp., Sunnyvale, CA, USA), SP (quaternary pump and degasser), DC (column compartment), and ED (electrochemical detector and gold electrode) units. Linuma et al. (2009) illustrated that the levoglucosan was separated by a Dionex CarboPac MA1 column (4 mm × 250 mm) with a CarboPac MA1 guard column (4 mm × 50 mm) with a sodium hydroxide solution (400 mM) eluent at a flow rate of 0.4 mL min<sup>-1</sup>. The detection limit was 0.002 mgL<sup>-1</sup> for levoglucosan. More details about this analyzer, especially for its calibration, were given by Engling et al. (2006).

A nondispersive infrared absorption TOC (Total Organic Carbon) analyzer (ET1020A) was used to quantify WSOC concentration in ambient PM<sub>2.5</sub> samples. Before analysis, the quartz filters were

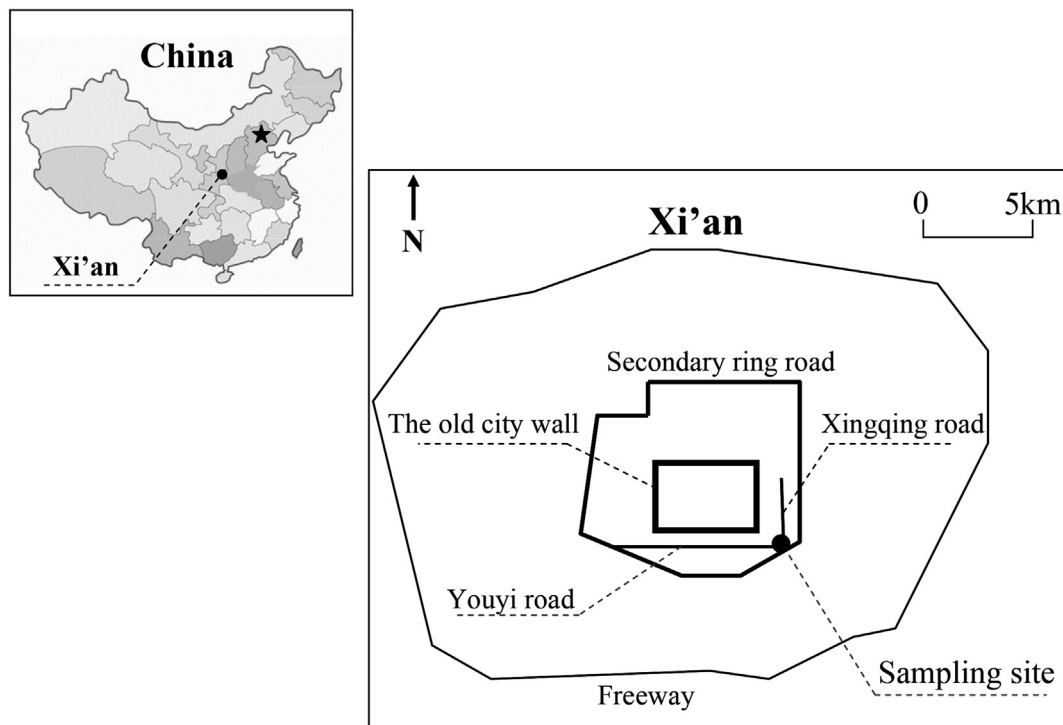


Fig. 1. Location of the sampling site.

extracted following the method of WS-ions pretreatment. Both WSOC and inorganic carbons in each liquid extracts were converted into carbon dioxide using chemical oxidation involving ammonium persulfate and UV light. These two kinds of carbon dioxide generated in the tube were imported to a nondispersive infrared inspection detector. The infrared absorption intensity is proportional to its concentration under a particular wavelength. The organic carbon concentration was calculated from the difference between a total carbon channel and inorganic carbon channel. The TOC analyzer was calibrated before and after the measurements with a series of sucrose standards (linear regression  $R = 0.9999$ ,  $N = 5$ ). Each sample was measured three times and the repeat errors were limited within 5%.

For thermal carbonaceous analysis (OC and EC), a  $0.5 \text{ cm}^2$  punch of each sample was analyzed using a DRI Model 2001 Thermal and Optical Carbon Analyzer (Atmoslytic Inc., Calabasas, CA, USA) following the IMPROVE TOR protocol (Chow et al., 1993, 2004). Four OC fractions (OC1, OC2, OC3, and OC4 at  $140^\circ\text{C}$ ,  $280^\circ\text{C}$ ,  $480^\circ\text{C}$ , and  $580^\circ\text{C}$ , respectively, in a non-oxidizing helium atmosphere), and three EC fractions (EC1, EC2, and EC3 at  $580^\circ\text{C}$ ,  $740^\circ\text{C}$ , and  $840^\circ\text{C}$ , respectively, in a 2% oxygen/98% helium atmosphere) were produced. During volatilization of organic carbon, part of organic carbon was converted pyrolytically to EC (this fraction of OC was named as OP) (Chow et al., 2004). Hence, the IMPROVE protocol defines OC as  $\text{OC1} + \text{OC2} + \text{OC3} + \text{OC4} + \text{OP}$  and EC as  $\text{EC1} + \text{EC2} + \text{EC3} - \text{OP}$ . The DRI Model 2001 analyzer was calibrated with known quantities of  $\text{CH}_4$  daily. Replicate analyses were the same as for water-soluble ions. Blank sample was also analyzed for correcting field samples. The detection limits for EC and OC were below  $1.0 \mu\text{g m}^{-3}$ , and the difference determined from replicate analyses was smaller than 5% for total carbon (TC) and was 10% for OC and EC. Additional quality assurance and quality control procedures were described in detail in Cao et al. (2003).

### 2.3. Absorption coefficient of WSOC

Absorbance ( $A$ ) of ambient and combustion sources  $\text{PM}_{2.5}$  filters were measured at wavelengths from 190 nm to 800 nm with UV–vis recording spectrophotometer (UV-6100s) with 10 cm optical paths of quartz cells in the individual solvent. Each solvent was extracted from 9 punches of ambient filters and a quarter of combustion sources filters in distilled-deionized water (50 mL and 25 mL) following the same method as WS-ions pretreatment. In this study, absorption spectra of water extracts of aerosols (representing bulk water-soluble organic carbon) have been used to assess the absorption coefficient ( $b_{\text{abs}}$ ) as described by Liu et al. (2013) and Srinivas and Sarin (2014). The  $b_{\text{abs}}$  was calculated according to:

$$b_{\text{abs}} = (A_{340} - A_{700}) \cdot (V_{\text{ext}} \cdot \text{Portions}) \cdot \ln(10) / (V_{\text{aero}} \cdot L)$$

In this equation,  $b_{\text{abs}}$  is expressed in the unit of  $\text{Mm}^{-1}$  (or  $10^{-6} \text{ m}^{-1}$ ). Earlier studies have documented strong UV-absorption of water-soluble BrC at 340–370 nm and the value of  $b_{\text{abs}}$  can be derived from spectroscopic data using the sample absorbance ( $A$ ) (Hecobian et al., 2010; Lukács et al., 2007; Chen and Bond, 2010; Liu et al., 2013, 2014). In the present study, we have calculated that the  $b_{\text{abs}}$  of 340 nm was the highest at varying wavelength (from 300 to 700 nm) relative to 700 nm. Therefore,  $A_{340}$  and  $A_{700}$  correspond to measured absorbance at 340 and 700 nm, respectively.  $V_{\text{ext}}$  refers to volume of the aqueous extract (50 mL and 25 mL) in which different portions of filter (1.2% for ambient samples and 25% for combustion sources samples) were used to extract and estimate the absorption signal for the full filter.  $V_{\text{aero}}$  corresponds to sampling volume and  $L$  is the path length of the cell (10 cm). We have used absorbance at 340 nm to estimate  $b_{\text{abs}}$  of light absorbing water-soluble organic carbon (also referred to as BrC). It is relevant to state that light absorption by OC in solvent extracts is underestimated by a factor of two than that of particulate OC (Liu et al.,

2013). During operation, each quartz cell was flushed by 0.6 N solution of HCl and distilled-deionized water. Prior to absorption measurements, the baseline of UV–Vis spectrometer should be zeroed using the Spectra-Suite software so that zero absorption was recorded at all wavelengths for distilled-deionized water (18.3 MΩ).

The relationship between wavelength-dependent AAC and  $b_{\text{abs}}$  of BrC in the aqueous extracts is described following Hecobian et al. (2010):

$$b_{\text{abs}} = K * \lambda^{-\text{AAC}}$$

here K refers to a constant value and  $\lambda$  denotes wavelength of BrC.

As described in Moosmüller et al. (2009, 2011), AAC can be calculated using the relationship between the ratio of the  $b_{\text{abs}}$  and two vacuum wavelengths  $\lambda_1$  and  $\lambda_2$ :

$$b_{\text{abs}}(\lambda_1)/b_{\text{abs}}(\lambda_2) = (\lambda_1/\lambda_2)^{-\text{AAC}}$$

which can then be solved for AAC:

$$\text{AAC} = -(\ln(b_{\text{abs}}(\lambda_1)) - \ln(b_{\text{abs}}(\lambda_2)))/(\ln(\lambda_1) - \ln(\lambda_2))$$

Justifying AAC values is a highly sensitive approach to classify the presence of BrC (Saleh et al., 2014; Sandradewi et al., 2008; Chen and Bond, 2010; Clarke et al., 2007; Lack and Cappa, 2010). The steep increase of ambient and combustion aerosol AAC values can also be used as a significance indicator for identifying specific BrC sources. A value between 1 and 2.9 for AAC was derived from coal burning aerosols and around 6–8 from biomass burning (Bond, 2001; Hecobian et al., 2010). Chen and Bond (2010) reported that higher AAC values (6.9–11.4) of BrC were from the incomplete biofuel burning in methanol extracts. The prominent difference in AAC values between the aged and fresh aerosols suggested that the formation mechanisms also played important roles in BrC absorption parameters (Zhang et al., 2011; Bones et al., 2010). AAC of BrC in the aqueous extracts of aerosols measured in the present study was similar to that of light absorbing matters in water-soluble organic carbon found in previous studies. As a consequence, the mass absorption efficiency of BrC ( $\text{m}^2\text{g}^{-1}$ ) is the ratio between  $b_{\text{abs-340}}$  ( $\text{Mm}^{-1}$ ) and mass concentration of WSOC ( $\mu\text{g}\text{m}^{-3}$ ).

### 3. Results and discussion

#### 3.1. Seasonal and diurnal variations of $b_{\text{abs}}$ , AAC, and MAC

Fig. 2 shows a scatter plot of  $b_{\text{abs}}$  and MAC against the wavelength ranged from 300 nm to 800 nm. The peaks of  $b_{\text{abs}}$  and MAC occurred at 340 nm in all the seasons except winter, verifying the presence of brown carbon (BrC) due to its prominent absorption at

this wavelength. The seasonal variations in  $b_{\text{abs}}$  (340 nm) were up to a factor of 4.7 and followed the sequence of winter ( $36.2 \text{ Mm}^{-1}$ ) > autumn ( $17.6 \text{ Mm}^{-1}$ ) > spring ( $10.8 \text{ Mm}^{-1}$ ) > summer ( $7.7 \text{ Mm}^{-1}$ ), indicating that the winter  $\text{PM}_{2.5}$  had a significant amount of BrC in comparison with other seasons. Earlier studies reported that biomass burning for heating in rural areas around Xi'an contributed significantly to PM (Shen et al., 2010, 2014; Zhang et al., 2014). The highest WSOC, levoglucosan, and  $\text{K}^+$  concentrations in winter also suggested the important contribution of biomass burning to BrC. Thus, BrC in  $\text{PM}_{2.5}$  was much higher in winter than other seasons. Earlier studies mainly focused on biomass or biofuel-dominated sources (corresponding to  $b_{\text{abs}}$  of  $8\text{--}15 \text{ Mm}^{-1}$ ) or fossil burning sources ( $\sim 3 \text{ Mm}^{-1}$ ). A wider range of  $b_{\text{abs}}$  at 300–500 nm wavelength ( $7.65\text{--}36.23 \text{ Mm}^{-1}$ ) investigated in this study than earlier ones showed various BrC sources and high BrC pollution during the sampling days (Liu et al., 2013; Zhang et al., 2013). MAC was the highest at 300 nm ( $7.1 \text{ m}^2\text{g}^{-1}$ ), and dropped rapidly to about zero near 500 nm, a phenomenon similar to what was found in Barnard et al. (2008), emphasizing that MAC was a sensitive parameter related to wavelength.

To assess the impact of BrC on light absorption by WSOC at 340 nm, correlation analysis was conducted between  $b_{\text{abs}}$  and WSOC. A strong correlation ( $R = 0.93$ ,  $P < 0.001$ ) was observed using all the samples (Fig. 3a), verifying BrC as the dominant absorption material in water-extracts and having similar sources to WSOC, as reported in previous studies (Hecobian et al., 2010; Zhang et al., 2011; Shen et al., 2014). Looking at the data separately for each season, the lowest correlation was observed in summer ( $R = 0.63$ ,  $P < 0.001$ ) and the highest in spring ( $R = 0.93$ ) (Fig. 3 b), implying more sophisticated sources of BrC and WSOC in summer than in other seasons. In fact, Hecobian et al. (2010) also found the lowest coefficient between  $b_{\text{abs}}$  and WSOC in summer at sites in Southeastern United State, which was due to fewer biomass burning activities in summer resulting of low levels WSOC. At the same time, more light absorbing secondary organic aerosols were formed from photochemical processes (Hecobian et al., 2010).

Temporal variations of optical parameters ( $b_{\text{abs}}$ , AAC, and MAC) and WSOC levels are shown in Fig. 4. The winter highest and the summer lowest  $b_{\text{abs}}$  and WSOC implied their complex sources. The  $b_{\text{abs}}$  showed a strong dependency on wavelength (as  $\lambda^{-5.4}$ ) and the highest AAC value was found in winter (5.7), confirming the heavy BrC loading in aqueous extracts in winter. The typical AAC values found in this study ranged from 4.8 to 6.7, which covered aged and fresh SOA and other primary combustion sources (such as coal burning, biofuel burning, and biomass burning). Thus, various BrC sources existed during the sampling days (Srinivas and Sarin, 2014; Cheng et al., 2011; Bones et al., 2010; Hecobian et al., 2010; Kirchstetter et al., 2004). The seasonal pattern of MAC (340 nm) exhibited a decreasing order of summer > spring >

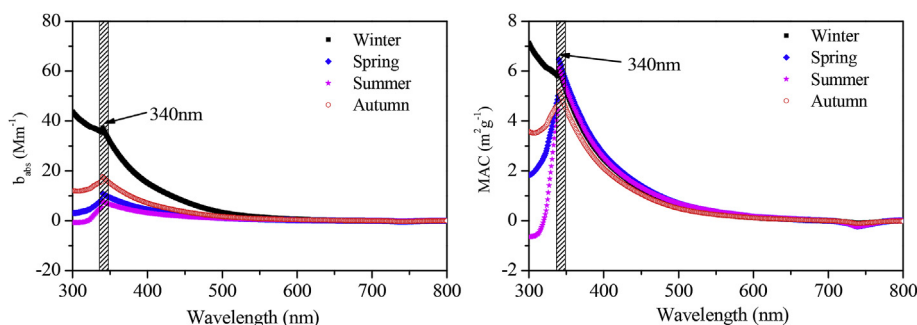


Fig. 2. Absorption coefficient ( $b_{\text{abs}}$ ) and mass absorption coefficient (MAC) of BrC as a function of wavelength ranging from 300 to 700 nm in different seasons (where  $\text{Mm}^{-1} = 10^{-6} \text{ m}^{-1}$ ).

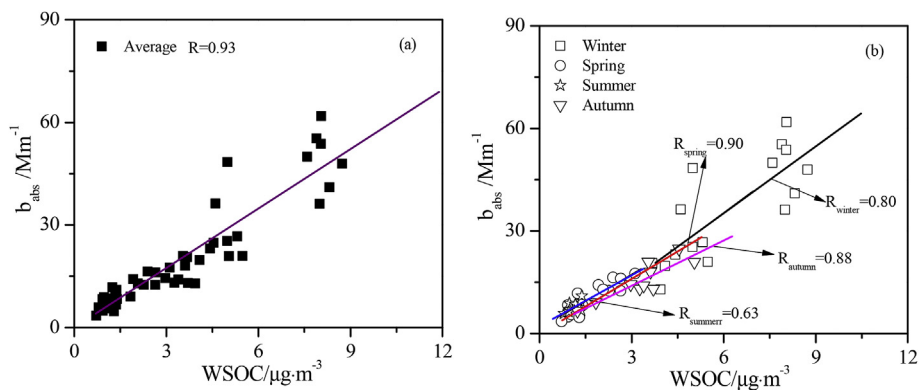


Fig. 3. Scatter plot for absorption coefficient ( $b_{\text{abs}}$ ) of light absorbing BrC at 340 nm and mass concentration of water-soluble organic carbon (WSOC): (a) all the data; and (b) seasonal data.

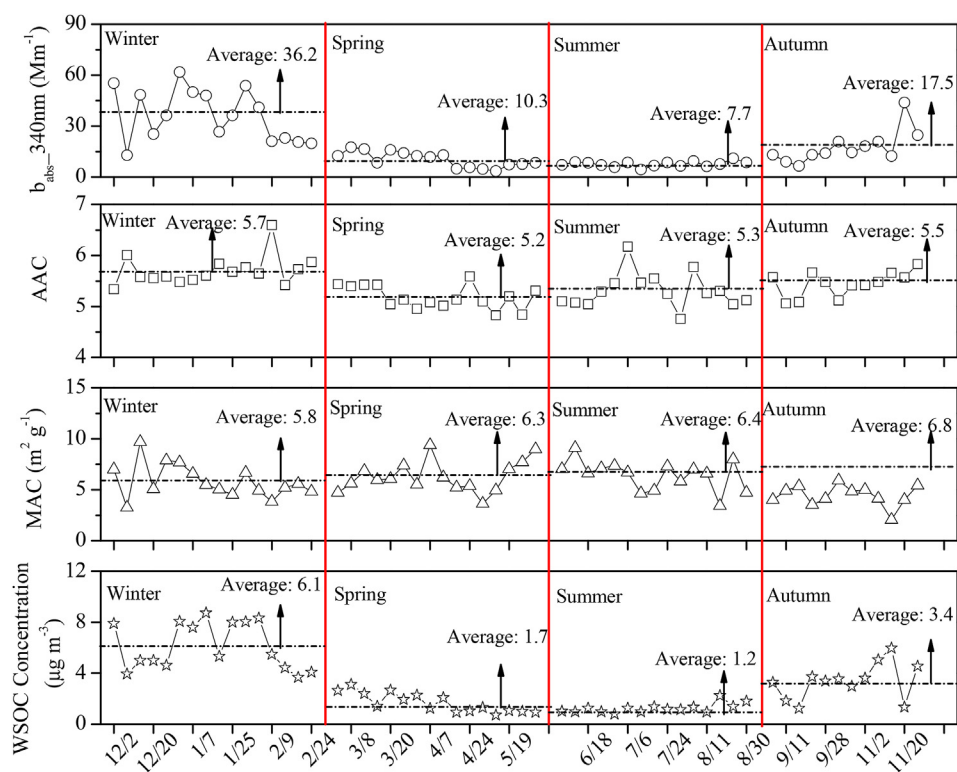


Fig. 4. Temporal variability of optical parameters ( $b_{\text{abs}}$ , AAC, and MAC) of BrC and WSOC concentrations during the sampling periods.

winter > autumn, slightly different from that of  $b_{\text{abs}}$ . It was noted that MAC had smaller seasonal variations, which was mainly because MAC value was not governed solely by absorbing efficient, but also influenced by WSOC concentration and aerosol mass distribution. For example, high summer MAC might also be partially caused by smaller mass median aerodynamic diameter of fine particles (Cheng et al., 2015).

### 3.2. BrC absorption properties in relation to chemical composition

Average concentrations of water soluble-ions, carbon species, and levoglucosan are listed in Table 1. The sum of  $\text{SO}_4^{2-}$ ,  $\text{NO}_3^-$ , and  $\text{NH}_4^+$  accounted for ~76.4% of the total ions concentration. To further investigate the contribution of SOC to OC, the EC-tracer method proposed by Turpin and Huntzicker (1995) was used to estimate SOC and primary organic carbon (POC) concentrations:

$$\text{SOC} = \text{OC}_{\text{tot}} - \text{EC} * (\text{OC}/\text{EC})_{\text{min}}, \text{ and } \text{POC} = \text{OC}_{\text{tot}} - \text{SOC}$$

where  $\text{OC}_{\text{tot}}$  is the total of OC, and  $(\text{OC}/\text{EC})_{\text{min}}$  is the minimum OC/EC ratio observed during the study period. The estimated SOC is the highest in winter ( $21.62 \mu\text{g m}^{-3}$ ), followed by autumn ( $9.84 \mu\text{g m}^{-3}$ ), spring ( $4.43 \mu\text{g m}^{-3}$ ), and summer ( $2.33 \mu\text{g m}^{-3}$ ). Moreover, the estimated seasonal average SOC accounted for about 43%, 31%, 21%, and 35% of organic matter (OM, estimated by  $1.6 * \text{OC}$ ) in the four seasons (winter, spring, summer, and autumn), respectively. These results appeared to be consistent with former studies (Zhang et al., 2015; Huang et al., 2014).

Absorbing sources can be grouped into two categories: primary BrC and SOC–BrC (Barnard et al., 2008). As shown in Fig. 5, significant correlations ( $R > 0.86$ ) were observed between  $b_{\text{abs}}$  and biomass emission tracers ( $\text{K}^+$  and levoglucosan), suggesting heavy

**Table 1**  
Seasonal average mass concentrations ( $\mu\text{g m}^{-3}$ ) of water-soluble inorganic ions, levoglucosan, and carbon species.

Concentration/ $\mu\text{g m}^{-3}$	Winter		Spring		Summer		Autumn	
	Average	SD	Average	SD	Average	SD	Average	SD
Na <sup>+</sup>	2.4	0.5	2.1	1.0	1.5	0.5	1.5	0.8
NH <sub>4</sub> <sup>+</sup>	10.3	3.9	4.1	2.9	5.0	2.5	6.1	2.5
K <sup>+</sup>	8.5	12.6	2.3	0.5	1.1	0.2	1.6	2.5
Mg <sup>2+</sup>	0.6	1.0	0.2	0.2	0.2	0.1	0.2	0.1
Ca <sup>2+</sup>	1.7	2.1	2.2	0.9	1.2	0.6	0.9	0.7
F <sup>-</sup>	0.5	0.3	0.1	0.1	0.1	0.0	0.2	0.2
Cl <sup>-</sup>	10.9	7.6	2.2	1.4	1.4	0.7	4.5	2.8
NO <sub>3</sub> <sup>-</sup>	16.0	7.6	5.3	5.1	5.7	4.0	9.7	5.1
SO <sub>4</sub> <sup>2-</sup>	30.8	12.0	13.2	7.9	16.5	7.5	17.4	7.8
OC	31.6	12.8	8.8	4.3	7.0	1.4	17.6	9.9
EC	11.1	4.2	4.9	1.9	5.1	1.4	8.7	2.4
SOC	21.6	10.9	4.4	3.1	2.3	0.8	9.8	8.5
WSOC	5.7	1.9	1.7	0.8	1.2	0.4	2.8	1.4
Levoglucosan	1.2	0.5	0.2	0.2	0.2	0.1	0.8	0.6

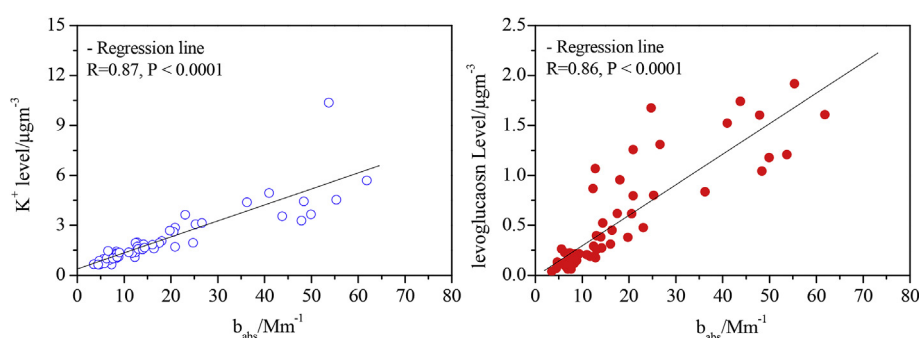


**Fig. 5.** Relationship between absorption coefficient ( $b_{\text{abs}}$ ) of BrC at 340 nm and the abundance of K<sup>+</sup> and levoglucosan.

absorbing impacts contributed from primary sources in this region. A large number of aromatic carbonyls, which are absorbing materials of BrC, existed in fresh biomass burning emissions (Desyaterik et al., 2013). Higher correlation coefficient between  $b_{\text{abs}}$  and POC in the four seasons (0.90, 0.83, 0.75, and 0.75 from spring to winter) also proved the significant contribution of primary emissions. The correlation coefficients between  $b_{\text{abs}}$  and SOC were higher in autumn, winter, and spring (0.93, 0.73, and 0.68), whereas it was much lower in summer (0.1), implying the lower SOC–BrC content in summer than other seasons. These seasonal differences in the relationship between  $b_{\text{abs}}$  and SOC illustrated seasonal dependent SOC formation mechanisms. As concluded from former studies, summer SOA was generated mainly from photochemical processes of ozone ( $\text{O}_3$ ) and hydroxyl radical (OH) initiated oxidation of various biogenic (such as isoprene,  $\alpha$ -pinene, and limonene) and anthropogenic (such as tetradecane, 1,3,5-trimethylbenzene, and naphthalene) precursors (Updyke et al., 2012; Cheng et al., 2011). In fact,  $\text{O}_3$  concentration was found to be the highest in summer over Xi'an (Wang et al., 2012). However, SOC formation through aqueous reaction is prevalent in winter in Xi'an under conditions of high relative humidity, low temperature, and strong  $\text{PM}_{2.5}$  acidity condition (Zhang et al., 2015). Our results highlighted that the formation of SOC–BrC influenced heavily on BrC optical properties, since most of SOC–BrC produced from aqueous reactions had stronger optical absorption than that produced from photochemical processes. Considering that BrC was measured through the water extract method in this study, the methanol extraction method should be applied in the future to verify the above conclusion.

### 3.3. Source identification of BrC in Xi'an

In this study, local sources  $\text{PM}_{2.5}$  samples, such as coal burning, maize straw smoldering in “Heated Kang”, and straw pellet burning were determined to identify the origins of ambient  $\text{PM}_{2.5}$  BrC. Table 2 shows the  $b_{\text{abs}}$  and AAC values of these three sources samples. The  $b_{\text{abs}}$  at 340 nm followed a decreasing order by maize straw smoldering ( $65,655 \text{ Mm}^{-1}$ ), straw pellet burning ( $682.1 \text{ Mm}^{-1}$ ), and coal burning ( $84.9 \text{ Mm}^{-1}$ ). The  $b_{\text{abs}}$  for maize straw smoldering is much higher than others, which verified that the smoldering or incompletely biomass burning produce abundant BrC. It was noted that  $b_{\text{abs}}$  sharply decreased from maize straw smoldering to straw pellet burning, indicating that oxygen-enriched combustion can reduce BrC emissions more effectively. As the maize straw smoldering in “Heated Kang” is the traditional way for winter heating from mid-November to mid-March the next year in rural areas around Xi'an, this can explain the much higher  $b_{\text{abs}}$  in winter than other seasons.

The AAC of coal burning samples ranged from 3.65 to 4.92, with an average of 4.38. The coal burning AAC was much smaller than those of the biomass burning (7.44) and straw pellet burning (6.78). As shown in Table 3, the biomass burning AAC in Xi'an was similar

**Table 2**  
Average values of AAC and  $b_{\text{abs}}$  of BrC in different combustion sources.

Source	AAC	$b_{\text{abs}}$ ( $\text{Mm}^{-1}$ )
Biomass burning (smoldering)	7.44	65,655
Straw briquette	6.78	682.1
Coal burning	4.38	84.9

**Table 3**  
Comparison of mass absorption coefficient (MAC) and Absorption Ångström coefficient (AAC) values of BrC between the present and earlier studies in literature.

Region	Source	Key observations	$\lambda$ (nm)	MAC ( $\text{m}^2 \text{g}^{-1}$ )	AAC	Reference
Xi'an, China	Ambient	Water-soluble BrC	340	5.38	5.33	This study
Xi'an, China	BBE <sup>a</sup>		340	–	7.44	
Xi'an, China	BBE <sup>a</sup> -Straw rods		340	–	6.78	
Xi'an, China	Coal burning		340	–	4.38	
Indo-Gangetic plain	BBE <sup>a</sup> /BFE <sup>b</sup>	Water-soluble BrC	365	$0.78 \pm 0.24$	$6.0 \pm 1.1$	Srinivas and Sarin, 2014
Bay of Bengal (IGP-outflow)	BBE <sup>a</sup> /BFE <sup>b</sup>	Water-soluble BrC	365	$0.4 \pm 0.1$	$9.1 \pm 2.5$	Srinivas and Sarin, 2013
Bay of Bengal (SEA-outflow)	BBE <sup>a</sup> /BFE <sup>b</sup>		365	$0.5 \pm 0.2$	$6.9 \pm 1.9$	2013
USA	BF-smoldering	Methanol/Water-soluble BrC	<400		7–16	Chen and Bond, 2010
Laboratory	freshly formed SOA <sup>c</sup>	Water-soluble SOA			8.6	Bones et al., 2010
	aged SOA <sup>c</sup>				–17.8	
					4.7	
Berkeley, California; San Francisco	mixed aerosol from combustion	Filter-based transmission measurements	350	5.0	1.0–2.5	Kirchstetter et al., 2004
Bay Area; outdoor burning of firewood	of lignite, hard coal, and biomass					
USA	BBE <sup>d</sup>	HULIS <sup>d</sup>	<300	~10		Sun et al., 2007
Mexico City Metropolitan	Ambient	MFRSR <sup>e</sup> -derived method	300	10.5		Barnard et al., 2008
			500	0		
Los-Angeles, USA	BBE <sup>a</sup>	Water-soluble BrC	365	0.71	$7.6 \pm 0.5$	Zhang et al., 2013
North America	BBE <sup>a</sup>	Photo-acoustic measurements	404	$0.82 \pm 0.43$	–	Lack et al., 2012
Beijing, China	BBE <sup>a</sup>	Filter-based transmission measurements	550	0.5	–	Yang et al., 2009
Beijing, China	BBE <sup>a</sup>	Filter-based transmission measurements	365	$1.8 \pm 0.2$ (summer)	$7.5 \pm 0.9$	Cheng et al., 2011
Beijing, China	BBE <sup>a</sup>	Filter-based transmission measurements	365	$0.7 \pm 0.2$ (winter)	$7.0 \pm 0.8$	Cheng et al., 2011
South-eastern US & Atlanta, Georgia	BBE <sup>a</sup>	Water-soluble BrC	365	$0.64$ (urban) & $0.58$ (rural)	$7 \pm 1$	Hecobian et al., 2010
Amazon basin	BBE <sup>a</sup>	HULIS	350	$-0.5-1.5$	$-6-7$	Hoffer et al., 2006
			–400			

Notes:

<sup>a</sup> Biomass burning emissions.

<sup>b</sup> Biofuel emissions.

<sup>c</sup> Secondary organic aerosols.

<sup>d</sup> HULIS humic-like substances.

<sup>e</sup> Multi-Filter Rotating Shadow-band Radiometer.

to the values in Bay of Bengal (SEA-outflow) (Srinivas and Sarin, 2013), Los-Angeles (Zhang et al., 2013), Beijing (Cheng et al., 2011), amazon basin (Hoffer et al., 2006), and South-eastern US & Georgia (Hecobian et al., 2010). Therefore, high AAC value can be taken as the markers of BrC emitted from biomass burning. It was noted that AAC (5.33) for ambient PM<sub>2.5</sub> BrC was in between coal combustion and biomass burning, implying that the contributors of ambient BrC were mainly from the mix of these two emissions.

Based on the data of BrC optical parameters in the present and earlier studies with various sources and mixing states, a few insights can be generated (Table 3). In this study, the mean MAC for water soluble compounds was  $5.8 \text{ m}^2 \text{g}^{-1}$ , which was similar to the study of Kirchstetter et al. (2004). The BrC sources in these two studies were also correlated with mixing sources of lignite, hard coal, and biomass burning. Sun et al. (2007) and Barnard et al. (2008) analyzed the highest MAC values (~10) at ultraviolet wavelength for combustion and humic-like organic aerosol (HULIS), inferring that the MAC value correlated with typical combustion sources and surface materials changing (e.g. coatings). Lower MAC values ( $0.5-1.8 \text{ m}^2 \text{g}^{-1}$ ) were observed in BrC collected from intense biomass burning or biofuel burning at the other sites in former studies, further illustrating that BrC over Xi'an was from complex sources.

AAC (7.44) for biomass burning in this study was similar to the values measured from fresh biomass burning and biofuel burning at other sites mentioned above. This indicated that the value of AAC from fresh biomass burning leads to a relative high value range (6–9) in comparison with coal burning. In this study, AAC of coal burning BrC was measured with an average value of ~4.4. In addition, another significant portion of ambient BrC was derived from

SOA, and Bones et al. (2010) reported that AAC for aged SOA BrC ranged from 4.7 to 5.3. One can conclude that aged SOA-BrC was abundant in our sampling period because AAC value (5.4) was close to the aged SOA AAC (4.7–5.3). However, seasonal source identification of BrC should be different for various emission sources. In winter, due to additional coal combustion and biomass burning emissions for heating, the BrC origin should be mainly from heating emissions and the formation of SOA. And winter AAC was likely fresh SOA mainly formed on the aqueous solutions with high loading of  $\text{NH}_4^+$ , preventing slow aging process of SOA reactions (Updyke et al., 2012; Zhang et al., 2015). In contrast, in summer when biomass burning was limited, aged SOC should be the main contributor to BrC, as supported by the summer AAC values.

#### 4. Conclusions

BrC in WSOC was investigated in PM<sub>2.5</sub> samples in Xi'an. Strong light absorption at 340 nm wavelength with a high  $b_{\text{abs}}$  of  $36.23 \text{ Mm}^{-1}$  was found in winter samples, implying abundance of BrC existing in the region. In contrast, summer  $b_{\text{abs}}$  was much lower than winter. The AAC values for BrC varied within a small range of 5.0–6.2 for all samples. Meanwhile, the positive relationship between WSOC and  $b_{\text{abs}}$  ( $R = 0.93$ ,  $P < 0.001$ ) illustrated that BrC was a significant component in WSOC. Biomass burning sources contributed significant amounts of BrC in winter and autumn, as evidenced by high levels of OC, levoglucosan, and  $\text{K}^+$ . SOC is also an important origin of BrC, especially in winter. Analysis of optical source profiles of BrC revealed that biomass burning smoldering had much higher  $b_{\text{abs}}$  than fossil burning and compressed biomass burning. Biomass burning constantly had higher AAC compared to

coal combustion.  $b_{\text{abs}}$  and AAC of PM<sub>2.5</sub> BrC in Xi'an were lower than those from biomass burning, slightly higher than those from coal burning, and close to those from SOC, indicating mixed origins of BrC in Xi'an. Compared with MAC and AAC values in other studies, it was found that winter SOA-BrC was likely freshly formed while summer SOA-BrC was from aged aerosols, which was likely caused by different formation mechanisms of SOC in different seasons. This study investigated BrC in WSOC only, and further studies should focus on BrC using the methanol extraction method. The relationship between organic compounds (such as aromatic hydrocarbon) and BrC should also be investigated to gain further insights of its origins.

## Acknowledgements

This research was supported by the National Natural Science Foundation of China (41573101), Natural Science Foundation of Shaanxi Province, China (2016ZDJC-22), the Fundamental Research Funding for Central Universities in China (xkjc2015002), and the Key Lab of Aerosol Chemistry & Physics of the Chinese Academy of Sciences (KLACP201501).

## References

- Andreae, M.O., Gelencser, A., 2006. Black carbon or brown carbon? The nature of light-absorbing carbonaceous aerosols. *Atmos. Chem. Phys.* 6, 3131–3148.
- Barnard, J.C., Volkamer, R., Kassianov, E.I., 2008. Estimation of the mass absorption cross section of the organic carbon component of aerosols in the Mexico City Metropolitan Area. *Atmos. Chem. Phys.* 8, 6665–6679.
- Bones, D.L., Henricksen, D.K., Mang, S.A., Gonsior, M., Bateman, A.P., Nguyen, T.B., Cooper, W.J., Nizkorodov, S.A., 2010. Appearance of strong absorbers and fluorophores in limonene-O<sub>3</sub> secondary organic aerosol due to NH<sub>4</sub><sup>+</sup>-mediated chemical aging over long time scales. *J. Geophys. Res.* 115 (D5), D05203.
- Bond, T.C., 2001. Spectral dependence of visible light absorption by carbonaceous particles emitted from coal combustion. *Geophys. Res. Lett.* 28 (21), 4075–4078.
- Cao, J.J., Lee, S.C., Ho, K.F., Zhang, X.Y., Zou, S.C., Fung, K., Chow, J.C., Watson, J.G., 2003. Characteristics of carbonaceous aerosol in Pearl river delta region, China during 2001 winter period. *Atmos. Environ.* 37, 1451–1460.
- Cao, J.J., Wu, F., Chow, J.C., Lee, S.C., Li, Y., Chen, S.W., An, Z.S., Fung, K.K., Watson, J.G., Zhu, C.S., Liu, S.X., 2005. Characterization and source apportionment of atmospheric organic and elemental carbon during fall and winter of 2003 in Xi'an, China. *Atmos. Chem. Phys.* 5, 3127–3137.
- Cao, J.J., Lee, S.C., Chow, J.G., Watson, J.G., Ho, R.J., Zhang, R.J., 2007. Spatial and seasonal distributions of carbonaceous aerosols over China. *J. Geophys. Res.* 112, D22S11.
- Cao, J.J., Zhu, C.S., Chow, J.C., Watson, J.G., Han, Y.M., Wang, G.H., Shen, Z.X., An, Z.S., 2009. Black carbon relationships with emissions and meteorology in Xi'an, China. *Atmos. Res.* 94, 194–202.
- Chakrabarty, R.K., Moosmüller, H., Chen, L.W., Lewis, K., Arnott, W.P., Mazzoleni, C., Dubey, M.K., Wold, C.E., Hao, W.M., Kreidenweis, S.M., 2010. Brown carbon in tar balls from smoldering biomass combustion. *Atmos. Chem. Phys.* 10, 6363–6370.
- Chen, Y., Bond, T.C., 2010. Light absorption by organic carbon from wood combustion. *Atmos. Chem. Phys.* 10, 1773–1787.
- Cheng, Y., He, K.B., Zheng, M., Duan, F.K., Du, Z.Y., Ma, Y.L., Tan, J.H., Yang, F.M., Liu, J.M., Zhang, X.L., Weber, R.J., 2011. Mass absorption efficiency of elemental carbon and water-soluble organic carbon in Beijing, China. *Atmos. Chem. Phys.* 11, 11497–11510.
- Cheng, C.L., Wang, G.H., Meng, J.J., Wang, Q.Y., Cao, J.J., Li, J.J., Wang, J.Y., 2015. Size-resolved airborne particulate oxalic and related secondary organic aerosol species in the urban atmosphere of Chengdu, China. *Atmos. Res.* 161–162, 134–142.
- Chow, J.C., Watson, J.G., Pritchett, L.C., Pierson, W.R., Frazier, C.A., Purcell, R.G., 1993. The dri thermal/optical reflectance carbon analysis system: description, evaluation and applications in U.S. Air quality studies. *Atmos. Environ.* 27 (8), 1185–1201.
- Chow, J.C., Watson, J.G., Chen, L.W.A., Arnott, W.P., Moosmüller, H., 2004. Equivalence of elemental carbon by thermal/optical reflectance and transmittance with different temperature protocols. *Environ. Sci. Technol.* 8, 4414–4422.
- Clarke, A., McNaughton, C., Kapustin, V., Shinozuka, Y., Howell, S., Dibb, J., Zhou, J., Anderson, B., Brekhovskikh, V., Turner, H., Pinkerton, M., 2007. Biomass burning and pollution aerosol over North America: organic components and their influence on spectral optical properties and humidification response. *J. Geophys. Res.* 112, D12S18.
- Desyaterik, Y., Sun, Y., Shen, X., Lee, T., Wang, X., Wang, T., Collett, J.L., 2013. Speciation of "brown" carbon in cloud water impacted by agricultural biomass burning in eastern China. *J. Geophys. Res.* 118, 7389–7399.
- Engling, G., Carrico, C.M., Kreidenweis, S.M., Collett, J.L., Day, D.E., Malm, W.C., Lincoln, E., Hao, W.M., Iinuma, Y., Herrmann, H., 2006. Determination of levoglucosan in biomass combustion aerosol by high-performance anion-exchange chromatography with pulsed amperometric detection. *Atmos. Environ.* 40, S299–S311.
- Feng, Y., Ramanathan, V., Kotamarthi, V.R., 2013. Brown carbon: a significant atmospheric absorber of solar radiation. *Atmos. Chem. Phys.* 13, 8607–8621.
- Hecobian, A., Zhang, X., Zheng, M., Frank, N., Edgerton, E.S., Weber, R.J., 2010. Water-Soluble Organic Aerosol material and the light-absorption characteristics of aqueous extracts measured over the Southeastern United States. *Atmos. Chem. Phys.* 10, 5965–5977.
- Hoffer, A., Gelencsér, A., Guyon, P., Kiss, G., Schmid, O., Frank, G.P., Artaxo, P., Andreae, M.O., 2006. Optical properties of humic-like substances (HULIS) in biomass-burning aerosols. *Atmos. Chem. Phys.* 6, 3563–3570.
- Huang, R.J., Zhang, Y., Bozzetti, C., Ho, K.F., Cao, J.J., Han, Y., Daellenbach, K.R., Slowik, J.G., Platt, S.M., Canonaco, F., Zotter, P., 2014. High secondary aerosol contribution to particulate pollution during haze events in China. *Nature* 514, 218–222.
- Kieber, R.J., Whitehead, R.F., Reid, S.N., Willey, J.D., Seaton, P.J., 2006. Chromophoric dissolved organic matter (CDOM) in rainwater, southeastern North Carolina, USA. *J. Atmos. Chem.* 54, 21–41.
- Kirchstetter, T.W., Novakov, T., Hobbs, P.V., 2004. Evidence that the spectral dependence of light absorption by aerosols is affected by organic carbon. *J. Geophys. Res.* 109, D21208.
- Kirchstetter, T.W., Thatcher, T.L., 2012. Contribution of organic carbon to wood smoke particulate matter absorption of solar radiation. *Atmos. Chem. Phys.* 12, 6067–6072.
- Lack, D.A., Cappa, C.D., 2010. Impact of brown and clear carbon on light absorption enhancement, single scatter albedo and absorption wavelength dependence of black carbon. *Atmos. Chem. Phys.* 10, 4207–4220.
- Lack, D.A., Langridge, J.M., Bahreini, R., Cappa, C.D., Middlebrook, A.M., Schwarz, J.P., 2012. Brown carbon and internal mixing in biomass burning particles. *PNAS* 109, 14802–14807.
- Iinuma, Y., Engling, G., Puxbaum, H., Herrmann, H., 2009. A highly resolved anion-exchange chromatographic method for determination of saccharidic tracers for biomass combustion and primary bio-particles in atmospheric aerosol. *Atmos. Environ.* 43, 1367–1371.
- Liu, J., Bergin, M., Guo, H., King, L., Kotra, N., Edgerton, E., Weber, R.J., 2013. Size-resolved measurements of brown carbon in water and methanol extracts and estimates of their contribution to ambient fine-particle light absorption. *Atmos. Chem. Phys.* 13, 12389–12404.
- Liu, J., Scheuer, E., Dibb, J., Ziemba, L.D., Thornhill, K., Anderson, B.E., Wisthaler, A., Mikoviny, T., Devi, J.J., Bergin, M., Weber, R.J., 2014. Brown carbon in the continental troposphere. *Geophys. Res. Lett.* 41 <http://dx.doi.org/10.1002/2013GL058976>.
- Lukács, H., Gelencsér, A., Hammer, S., Puxbaum, H., Pio, C., Legrand, M., Kasper-Giebl, A., Handler, M., Limbeck, A., Simpson, D., Preunkert, S., 2007. Seasonal trends and possible sources of brown carbon based on 2-year aerosol measurements at six sites in Europe. *J. Geophys. Res.* 112, D23S18.
- Moosmüller, H., Chakrabarty, R.K., Arnott, W.P., 2009. Aerosol light absorption and its measurement: a review. *J. Quant. Spectrosc. Radiat. Transf.* 110, 844–878.
- Moosmüller, H., Chakrabarty, R.K., Ehlers, K.M., Arnott, W.P., 2011. Absorption Ångström coefficient, brown carbon, and aerosols: basic concepts, bulk matter, and spherical particles. *Atmos. Chem. Phys.* 11, 1217–1225.
- Sandradewi, J., Prevot, A.S.H., Alfarra, M.R., Sztat, S., Wehrl, M.N., Ruff, M., 2008. Comparison of several wood smoke markers and source apportionment methods for wood burning particulate mass. *Atmos. Chem. Phys.* 8, 8091–8118.
- Saleh, R., Hennigan, C.J., McMeeking, G.R., Chuang, W.K., Robinson, E.S., Coe, H., Donahue, N.M., Robinson, A.L., 2013. Absorptivity of brown carbon in fresh and photo-chemically aged biomass-burning emissions. *Atmos. Chem. Phys.* 13, 7683–7693.
- Saleh, R., Robinson, E.S., Tkacik, D.S., Ahern, A.T., Liu, S., Auken, A.C., 2014. Brownness of organics in aerosols from biomass burning linked to their black carbon content. *Nature* 7, 647–650.
- Shen, Z.X., Cao, J.J., Arimoto, R., Zhang, R.J., Jie, D.M., Liu, S.X., Zhu, C.S., 2007. Chemical composition and source characterization of spring aerosol over Horqin sand land in northeastern China. *J. Geophys. Res.* 112, D14315.
- Shen, Z.X., Arimoto, R., Cao, J.J., Zhang, R.J., Li, X.X., Du, N., Okuda, T., Nakao, S., Tanaka, S., 2008. Seasonal variations and evidence for the effectiveness of pollution controls on water-soluble inorganic species in total suspended particulates and fine particulate matter from Xi'an, China. *J. Air Waste Manag. Assoc.* 58, 1560–1570.
- Shen, Z.X., Cao, J.J., Arimoto, R., Han, Z.W., Zhang, R.J., Han, Y.M., Liu, S.X., Okuda, T., Nakao, S., Tanaka, S., 2009. Ionic composition of TSP and PM<sub>2.5</sub> during dust storms and air pollution. *Atmos. Environ.* 43, 2911–2918.
- Shen, Z.X., Cao, J.J., Arimoto, R., Han, Y.M., Zhu, C.S., Tian, J., Liu, S.X., 2010. Chemical characteristics of fine particles (PM<sub>1</sub>) from Xi'an, China. *Aerosol Sci. Technol.* 44, 461–472.
- Shen, Z.X., Cao, J.J., Zhang, L.M., Liu, L., Zhang, Q., Li, J., Han, Y.M., Zhu, C.S., Zhao, Z.Z., Liu, S.X., 2014. Day–night differences and seasonal variations of chemical species in PM<sub>10</sub> over Xi'an, northwest China. *Environ. Sci. Pollut. Res.* 21, 3697–3705.
- Srinivas, B., Sarin, M.M., 2013. Light absorbing organic aerosols (brown carbon) over the tropical Indian Ocean: impact of biomass burning emissions. *Environ. Res.* 8 (4), 044042.
- Srinivas, B., Sarin, M.M., 2014. Brown carbon in atmospheric outflow from the Indo-

- Gangetic Plain: mass absorption efficiency and temporal variability. *Atmos. Environ.* 89, 835–843.
- Sun, H., Biedermann, L., Bond, T.C., 2007. Color of brown carbon: a model for ultraviolet and visible light absorption by organic carbon aerosol. *Geophys. Res. Lett.* 34, L17813.
- Sun, J., Shen, Z., Cao, J., Zhang, L., Wu, T., Zhang, Q., Yin, X., Lei, Y., Huang, Y., Huang, R.J., Liu, S., 2017. Particulate matters emitted from maize straw burning for winter heating in rural areas in Guanzhong Plain, China: current emission and future reduction. *Atmos. Res.* 184, 66–76.
- Tian, J., Chow, J.C., Cao, J., Han, Y., Ni, H., Chen, L.W.A., Wang, X., Huang, R., Moosmüller, H., Watson, J.G., 2015. A biomass combustion chamber: design, evaluation, and a case study of wheat straw combustion emission tests. *Aerosol Air Qual. Res.* 15 (5), 2104–2114.
- Turpin, B.J., Huntzicker, J.J., 1995. Identification of secondary organic aerosol episodes and quantitation of primary and secondary organic aerosol concentrations during scaqs. *Atmos. Environ.* 29, 3527–3544.
- Updyke, K.M., Nguyen, T.B., Nizkorodov, S.A., 2012. Formation of brown carbon via reactions of ammonia with secondary organic aerosols from biogenic and anthropogenic precursors. *Atmos. Environ.* 63, 22–31.
- Wang, X., Shen, Z.X., Cao, J.J., Zhang, L.M., Liu, L., Li, J.J., Liu, S.X., Sun, Y.F., 2012. Characteristics of surface ozone at an urban site of Xi'an in Northwest China. *J. Environ. Monit.* 14, 116.
- Yang, M., Howell, S.G., Zhuang, J., Huebert, B.J., 2009. Attribution of aerosol light absorption to black carbon, brown carbon, and dust in China – interpretations of atmospheric measurements during EAST-AIRE. *Atmos. Chem. Phys.* 9, 2035–2050.
- Zhang, X.L., Lin, Y.H., Surratt, J.D., Zotter, P., Prevot, A.S., Webber, R.J., 2011. Light-absorbing soluble organic aerosol in Los Angeles and Atlanta: a contrast in secondary organic aerosol. *Geophys. Res. Lett.* 38, L21810.
- Zhang, X.L., Lin, Y.H., Surratt, J.D., Webber, R.J., 2013. Sources, composition and absorption Ångström exponent of light-absorbing organic components in aerosol extracts from the Los Angeles basin. *Environ. Sci. Technol.* 47 (8), 3685–3693.
- Zhang, T., Cao, J.J., Chow, J.C., Shen, Z.X., Ho, K.F., Ho, S.S.H., Liu, S.X., Han, Y.M., Watson, J.G., Wang, G.H., Huang, R.J., 2014. Characterization and seasonal variations of levoglucosan in fine particulate matter in Xi'an, China. *J. Air Waste Manage. Assoc.* 64 (11), 1317–1327.
- Zhang, Q., Shen, Z.S., Cao, J.J., Zhang, R.J., Zhang, L.M., Huang, R.J., Zheng, C.J., Wang, L.Q., Liu, S.X., Xu, H.M., Zheng, C.L., 2015. Variations in PM<sub>2.5</sub>, TSP, BC, and trace gases (NO<sub>2</sub>, SO<sub>2</sub>, and O<sub>3</sub>) between haze and non-haze episodes in winter over Xi'an, China. *Atmos. Environ.* 112, 64–71.
- Zhu, C.S., Cao, J.J., Tsai, C.J., Shen, Z.X., Liu, S.X., Huang, R.J., Zhang, N.N., Wang, P., 2016. The rural carbonaceous aerosols in coarse, fine, and ultrafine particles during haze pollution in northwestern China. *Environ. Sci. Pollut. Res.* 23 (5), 4569–4575.